

# Compact, Field-Portable Lens-free Microscope using Superresolution Spatio-Spectral Light-field Fusion

Farnoud Kazemzadeh  
Emily Kuang  
Alexander Wong

University of Waterloo, ON, Canada  
University of Waterloo, ON, Canada  
University of Waterloo, ON, Canada

## Abstract

We present a compact, field-portable lens-free microscope based on the principle of spatio-spectral light-field fusion. This is the first time a device of this kind has been introduced whereby both superresolution and signal-to-noise ratio are enhanced via the marriage of synthetic aperture imaging and spectral light-field fusion holography, culminating in a system that is self-contained and field-portable while achieving high resolution, contrast, strong signal fidelity, and ultra-wide field-of-view. The active spatio-spectral illumination is accomplished in the presented microscope by arranging a series of pulsing LEDs emitting at different spectral wavelengths in a specific spatial formation. To demonstrate the performance of the presented microscope, the system was used to observe two histology samples: a bovine lung, and corn stem. The imaging results demonstrate the ultra-wide field-of-view advantage of the presented microscope over any other system of its kind, thus enabling for acquisition of the entire sample without the need for scanning, while producing high-resolution, high-contrast microscopy images (168 megapixels in the current system) that makes it well-suited for scientific and clinical examinations.

## 1 Introduction

Histology, the study of anatomy of tissues of plants and animals at the cellular level, is most often performed in the confines of a laboratory environment using large tabletop devices with high cost and complexity. With significant advances in computing power, new computational imaging techniques have shown considerable promise in simplifying and miniaturizing various traditionally complex and laborious imaging tasks. Of particular interest in the research community is the notion of lens-free microscopy, which has gained tremendous amount of traction as an enabler for large-scale scientific imaging. Lens-free microscopy is particularly advantageous for applications such as digital histology due to its capability of imaging a very large field-of-view (FOV). Additionally, lens-free microscopes are robust and inherently compact due to the lack of optical elements, therefore lending themselves to be used as a portable device [1].

The resolution and signal-to-noise ratio (SNR) achieved using lens-free microscopy can be improved beyond the inherent limits that are imposed primarily by the detector, as the pixel size of the detector dictates the spatial resolution while the sensitivity of the detector plays a large role in SNR. There are three main techniques for increasing the spatial resolution and SNR in lens-free microscopy: 1) light-field encoding magnification, 2) aperture scanning, and 3) wavelength scanning. The magnification of the light-field encoding can be achieved by placing the sample further away from the detector and closer to the light source [2]. Aperture scanning can be achieved by introducing sub-pixel shifts when capturing a series of light-field encodings of the same sample, which in turn creates a large synthetic aperture, thus increasing the resolution by an order of magnitude [3]. Finally, wavelength scanning can be achieved illuminating a sample with light at different wavelengths, with the appropriate combination of which would result in enhanced resolution and SNR [4, 5].

In this paper, we present a new, first-of-its-kind, lens-free microscope which combines aperture scanning and wavelength scanning into an integrated, compact, field-portable device capable of enhanced resolution, SNR, and ultra-wide field-of-view for a specific application of microscopy, namely digital histology. The device is designed and fabricated with ease-of-use in mind. It can accommodate any histology sample and can enable large-scale histology visualization in quasi-real-time.

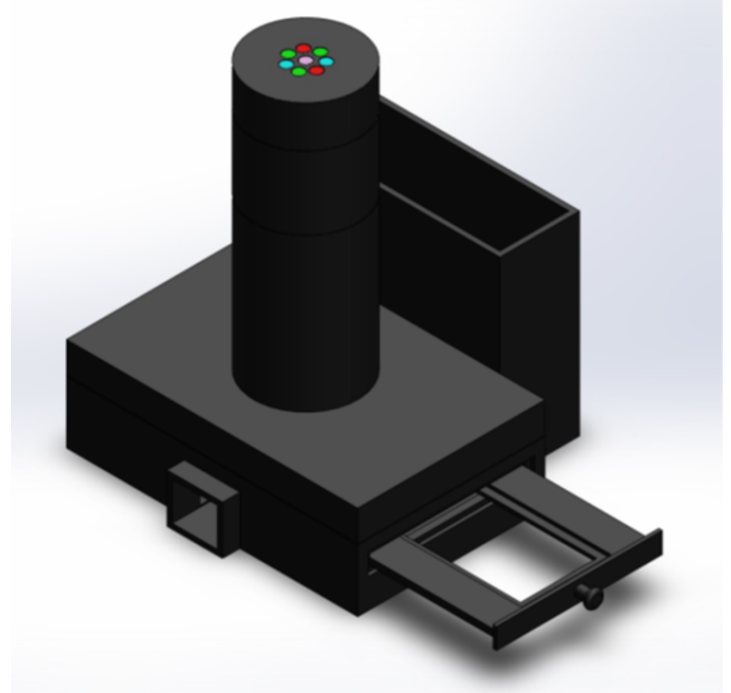


Fig. 1: 3D CAD render of the portable, lens-free, spatio-spectral light-field fusion microscope.

## 2 Methodology

The instrument, shown in Figure 1, consists of series of red, green, and blue light emitting diodes (LEDs) randomly placed in a honeycomb pattern. The LEDs are situated such that they all fully illuminate the 10.5 megapixel monochromatic detector. The sample is placed directly on the detector active area at a distance of  $< 1$  mm which would result in an ultra-wide field-of-view on the order of the active area of the detector,  $\sim 30$  mm<sup>2</sup> in this case. The light-field encodings at each wavelength and illumination location are sequentially captured by controlling the pulsation of the LEDs using an Arduino microcontroller. The instrument is encased in a 3D printed housing which allows for complete field-portability and autonomy from any laboratory environment. The sample can be loaded using a convenient tray and can handle different microscope slide models.

The captured spatio-spectral light-field encodings are computationally fused to reconstruct a fused object light-field (from which microscopy images at any depth can be obtained) using an extension on the Bayesian-based spectral fusion technique first presented by [4, 6] and later improved upon in [5], which can be described as follows. The fused object light-field (denoted by  $q_{x,y,z}$ ) can be computed as the subspace projection of the most probable object light-field (denoted by  $f_{x,y,z,\lambda}$ ) given the interferometric light-field encoding formed by combining a set of interferometric light-field encoding acquisitions made at different sub-pixel offsets and different wavelengths by the spatio-spectral light-field fusion microscopy system (denoted by  $g_{x,y,\lambda}^{ss}$ ):

$$\hat{q}_{x,y,z} = \int v_{\lambda} \left\{ \operatorname{argmax}_{f_{x,y,z,\lambda}} p \left( g_{x,y,\lambda}^{ss} | f_{x,y,z,\lambda} \right) p(f_{x,y,z,\lambda}) \right\} d\lambda, \quad (1)$$

where  $p \left( g_{x,y,\lambda}^{ss} | f_{x,y,z,\lambda} \right)$  represent the likelihood term and  $p(f_{x,y,z,\lambda})$  represent the prior term. Based on quantum photon emission statis-

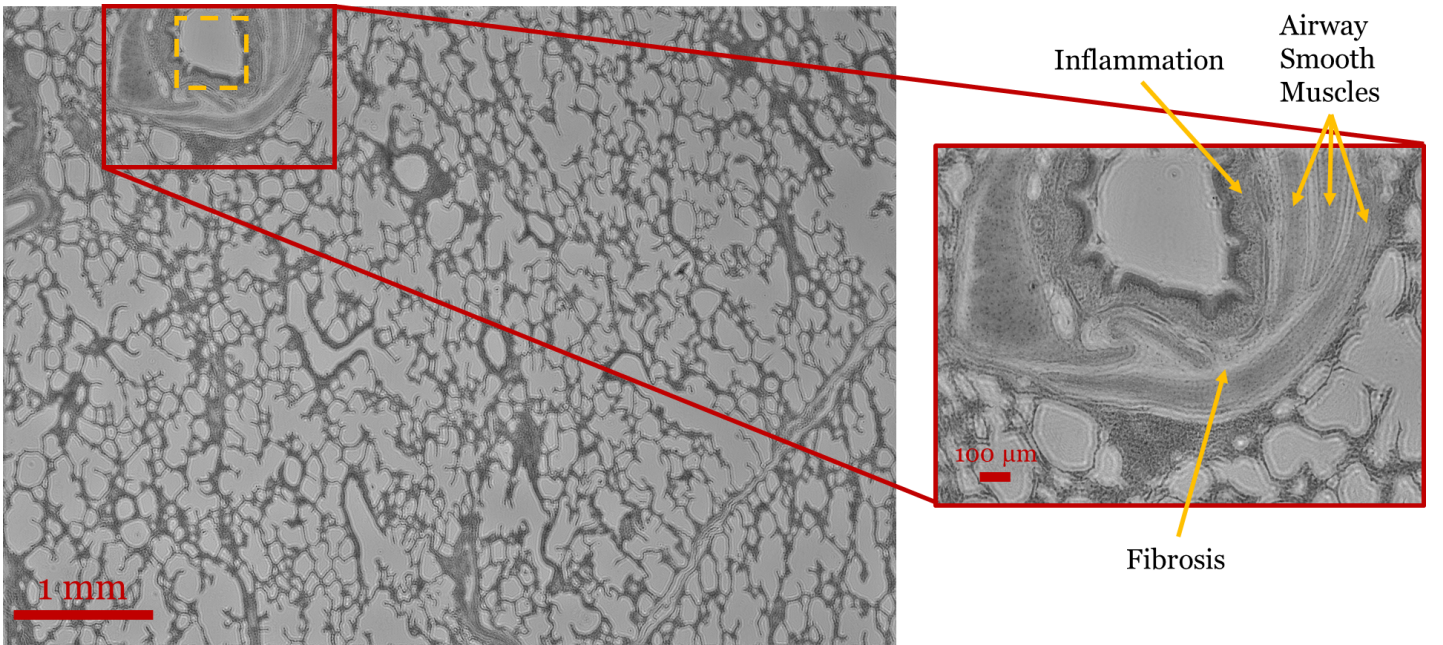


**Fig. 2:** Inflammation of asthmatic lung. The zoomed-in image shows various attributes associated with the inflammation such as the infiltration of the inflammatory cells, thickened and increased airway smooth muscles, and severe subepithelial fibrosis. For reference scales bars are included on the set of images and the field-of-view of a 40X microscope objective is shown in dashed orange box.

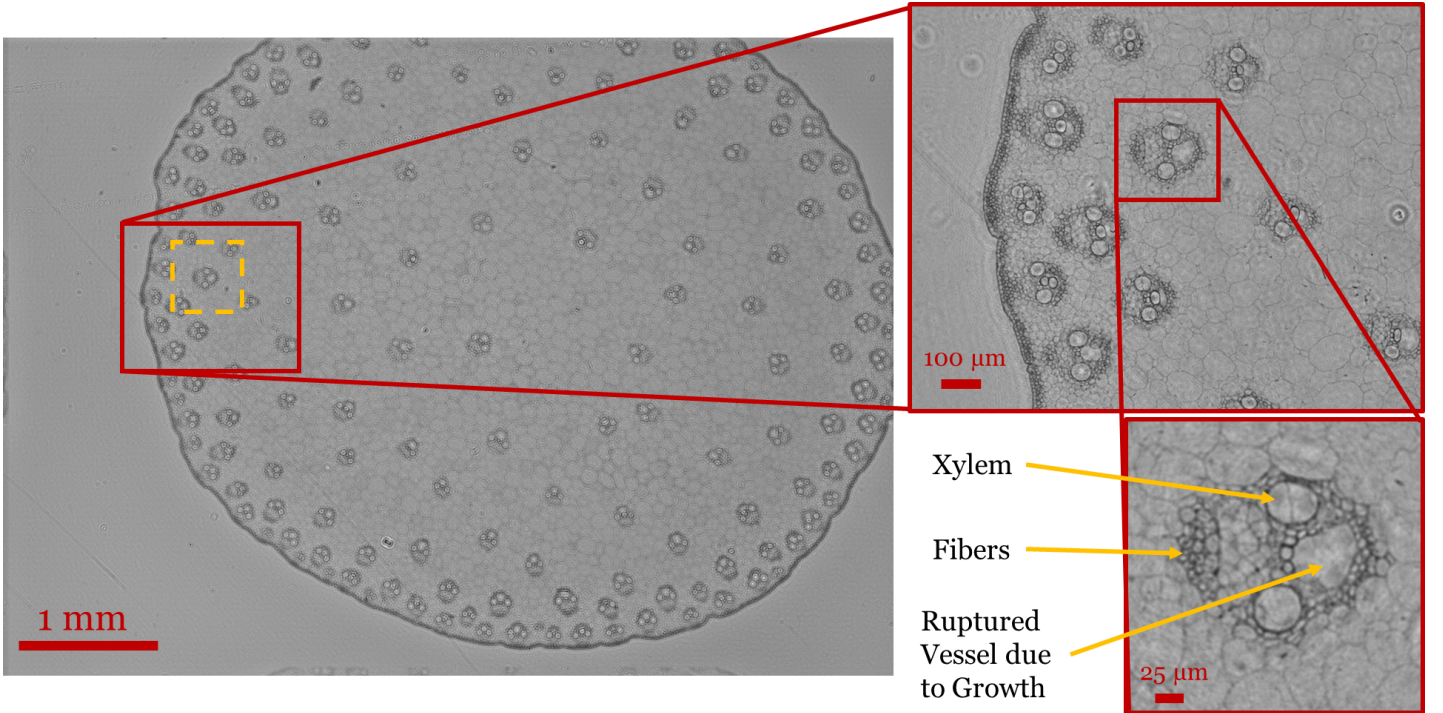


**Fig. 3:** A cross-section of the stem of a corn plant is shown in its entirety. Through two zoom levels various attributes at the cellular level can be observed. The Xylem which is the nutrient highway and the fibers in the plant can be observed. Also worth noting is that the crown of the plant can be observed via the ruptured vessels. For reference scales bars are included on the set of images and the field-of-view of a 40X microscope objective is shown in dashed orange box.

tics, the likelihood  $p(g_{x,y,\lambda}^{ss} | f_{x,y,z,\lambda})$  can be expressed by

$$p(g_{x,y,\lambda}^{ss} | f_{x,y,z,\lambda}) = \frac{\prod_{x \in X} \prod_{y \in Y} \prod_{z \in Z} \left( \mathfrak{F}^{-1} \left\{ \frac{H_{z,\lambda}^a}{H_{z,\lambda}^d} \mathfrak{F} \{ f_{x,y,z,\lambda} \} \right\} \right)_{x,y,\lambda}^{ss} e^{-\left( \mathfrak{F}^{-1} \left\{ \frac{H_{z,\lambda}^a}{H_{z,\lambda}^d} \mathfrak{F} \{ f_{x,y,z,\lambda} \} \right\} \right)_{x,y,\lambda}^{ss}}}{g_{x,y,\lambda}^{ss}!} \quad (2)$$

where  $\mathfrak{F}$  and  $\mathfrak{F}^{-1}$  represent the forward and inverse Fourier transform, respectively,  $H_{z,\lambda}^a$  represents the aberration transfer function, and  $H_{z,\lambda}^d$  represents the Rayleigh-Sommerfeld diffraction transfer function. Based on the assumption of  $f_{x,y,z,\lambda}$  being a nonstationary stochastic process, the prior  $p(f_{x,y,z,\lambda})$  can be expressed by

$$p(f_{x,y,z,\lambda}) = \prod_{x \in X} \prod_{y \in Y} \prod_{z \in Z} e^{-\frac{(f_{x,y,z,\lambda} - E(f_{x,y,z,\lambda}))^2}{2\tau^2}} \quad (3)$$

where  $E(f_{x,y,z,\lambda})$  denotes the nonstationary expectation and  $\tau^2$  denotes the variance.

### 3 Results and Discussion

To demonstrate the efficacy of the presented compact, field-portable lens-free microscope, digital histology was performed using the instrument on two different histology samples: i) bovine inflamed lung (see Figure 2), and ii) corn plant stem (see Figure 3). The microscopy images produced using the presented system in this study are 168 mega-pixels in size, resulting in a 16-fold increase compared to the 10.5 megapixel monochromatic detector used in the system. In Figure 2 a large area of the pathology sample can be observed and with it, many features of interest. In the zoomed-in image, the inflammation of the respiratory tract can clearly be ob-

served along with thickening or scarring (fibrosis) of the connective tissue in the airway smooth muscles. The major causes of the inflammation of lungs are asthma and chronic obstructive pulmonary disease [7].

Figure 3 shows the histology of a stem of a corn plant in its entirety. The epidermis, the outer layer of the sample, as well as the cuticles, cells comprising the epidermis, are clearly observed and can be enumerated. Furthermore, the cortex, the webbed structure within the sample, can be observed which is where the plant stores its nutrients required for photosynthesis. Through two zoom levels the vascular bundle can be observed. The water and ions within the plant are carried via the xylems which can be observed in the vascular bundle. Performing histology on plants in this manner can be beneficial in gauging health of the plant in one acquisition and may allow for estimating the yield or the crop.

For comparison, the field-of-view of a conventional, lab-based light microscope at 40X is shown in both Figures 2 and 3. It is clear that inspection of the entire histology slide with a conventional microscope is going to be a process which is cumbersome, time-consuming, and error prone.

## 4 Conclusions

In this paper, a compact, field-portable lens-free microscope based on the principles of spatio-spectral light-field fusion was introduced for the first time. The system was demonstrated to perform histology comparable to its lab-grade counterparts in image quality, while not being limited to the laboratory environment. A histopathology sample of a inflamed lung and a histology sample of corn plant stem were imaged. In both examples, the superior ultra-wide field-of-view of the instrument is significant as it allows for examining the samples in their entirety only after a single imaging session. The quality of the images allows for the appropriate examination and possible diagnosis.

## Acknowledgments

This work was supported by the Natural Sciences and Engineering Research Council of Canada, Canada Research Chairs Program, and the Ontario Ministry of Research and Innovation. The authors would like to thank their industry partner Lumalytics Inc.

## References

- [1] Tseng, F., Mudanyali, O., Oztoprak, C., Isikman, S.O., Sen-can, I., Yaglidere, O. and Ozcan, A., Lensfree microscopy on a cellphone, *Lab on a Chip* 10(14) 1787-1792 (2010).
- [2] Noom, D.W.E., Eikema, K.S.E. and Witte, S. Lensless phase contrast microscopy based on multiwavelength Fresnel diffraction, *Opt. Lett.* 39(2) 193-196 (2014).
- [3] Isikman, S.O., Greenbaum, A., Luo, W., Coskun, A.F., Ozcan, A. Giga-Pixel Lensfree Holographic Microscopy and Tomography Using Color Image Sensors, *PLoS ONE* 7(9), e45044 (2012).
- [4] Kazemzadeh, F., Jin, C., Molladavoodi, S., Mei, Y., Emelko, M.B., Gorbet, M.B. and Wong, A. Lens-free spectral light-field fusion microscopy for contrast- and resolution-enhanced imaging of biological specimens, *Opt. Lett.* 40(16), 3862-3865 (2015).
- [5] Kazemzadeh, F. and Wong, A., Lens-free Multi-Laser Spectral Light-Field Fusion Microscopy. *Vision Letters* 1(1) VL102 (2015).
- [6] Wong, A., Kazemzadeh, F., Jin, C., and Wang, X.Y. Bayesian-based aberration correction and numerical diffraction for improved lensfree on-chip microscopy of biological specimens, (*Opt. Lett.*) 40(10), 2233-2236 (2015).
- [7] Barnes, P.J., Similarities and differences in inflammatory mechanisms of asthma and COPD, *Breathe* 7(3), 229-238 (2011).